Stability Analysis and Dynamics Preserving Non-Standard Finite Difference Schemes for a Malaria Model

R Anguelov[1], Y Dumont[2], J M-S Lubuma[1]*, E Mureithi[1]
[1]Department of Mathematics and Applied Mathematics
University of Pretoria, Pretoria 0002, South Africa
[2] CIRAD-Umr AMAP, F-34398 Montpellier, France
*Contributor: jean.lubuma@up.ac.za

ICM 2010 International Congress of Mathematicians
HYDERABAD • INDIA
19-27 August 2010

Abstract

We extend the results in [2] by proving the GAS of the DFE and specifying the region of possible backward bifurcation. Furthermore, we design a nonstandard finite difference (NSFD) scheme, which is dynamically consistent with the continuous model.

1 The model

Fig. 1, Table 1 and Table 2 correspond to the model:

$$\begin{aligned}
\frac{dS_h}{dt} &= \Lambda_h + \psi_h N_h + \rho_h R_h - c(N_h,N_v)\beta_{hv} I_v S_h - f_h(N_h) S_h, && (1)\\
\frac{dE}{dt} &= c(N_h,N_v)\beta_{hv} I_v S_h - \nu_h E_h - f_h(N_h) E_h, && (2)\\
\frac{dI_h}{dt} &= \nu_h E_h - [\gamma_h + f_h(N_h) + \delta] I_h, && (3)\\
\frac{dR_h}{dt} &= \gamma_h I_h - \rho_h R_h - f_h(N_h) R_h, && (4)\\
\frac{dS_v}{dt} &= \psi_v N_v - c(N_h,N_v)(\beta_{vh} I_h + \tilde\beta_{vh} R_h) S_v - f_v(N_v) S_v, && (5)\\
\frac{dE_v}{dt} &= c(N_h,N_v)[\beta_{vh} I_h + \tilde\beta_{vh} R_h] S_v - \nu_v E_v - f_v(N_v) E_v, && (6)\\
\frac{dI_v}{dt} &= \nu_v(t) E_v - f_v(N_v) I_v && (7)
\end{aligned}$$

where

$$\begin{aligned}
f_h &= \mu_{1h} + \mu_{2h} N_h, \quad f_v = \mu_{1v} + \mu_{2v} N_v,\\
N_h &= S_h + E_h + I_h + R_h, \quad N_v = S_v + E_v + I_v,\\
c(N_h,N_v) &= \frac{\sigma_v \sigma_h}{\sigma_h N_h + \sigma_v N_v}.
\end{aligned}$$

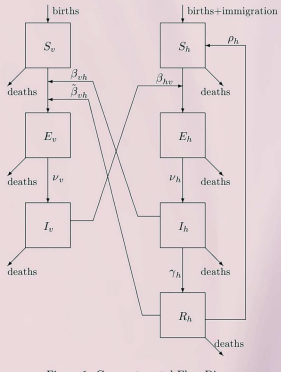

Figure 1: Compartmental Flow Diagram

Unbounded biologically feasible region:

$$\mathcal{D} = \{(\ S_h \quad E_h \quad I_h \quad R_h \quad S_v \quad E_v \quad I_v\ ) \in \mathbb{R}^7_+\}.$$

Conservation laws for vector and host:

$\frac{dN_v}{dt} = (\psi_v - \mu_{1v} - \mu_{2v} N_v) N_v$ with GAS equilibrium $N_v^* = \frac{\psi_v - \mu_{1v}}{\mu_{2v}}$.

$$\underline{N}_h(t) \le N_h(t) \le \overline{N}_h(t) \qquad (9)$$

with, $\overline{N}_h(t)$ and $\underline{N}_h(t)$ being suitable "upper" and "lower" solutions, equilibrium

$$\begin{aligned}
N_h^* &= (\psi_h - \mu_{1h} + \sqrt{(\psi_h - \mu_{1h})^2 + 4\mu_{2h}\Lambda_h})/2\mu_{2h} \text{ when } \delta_h = 0\\
N_h^\# &= (\psi_h - \mu_{1h} - \delta_h + \sqrt{(\psi_h - \mu_{1h} - \delta_h)^2 + 4\mu_{2h}\Lambda_h})/2\mu_{2h} \text{ when } \delta_h \neq 0
\end{aligned}$$

Disease free equilibrium (DFE):

$$DFE = (N_h^*, 0, 0, 0, N_v^*, 0, 0).$$

Humans		*Mosquito*	
S_h :	Number of susceptible humans	S_v :	Number of susceptible mosquito
E_h :	Number of exposed humans	E_v :	Number of exposed mosquito
I_h :	Number of infective humans	I_v :	Number of infective mosquito
R_h :	Number of recovered (immune and asymptomatic, but slightly infectious) humans		

Table 1: The state variables of the model (1) (7)

	Set 1	Set 2	Set 3
R_0	0.9503	0.9898	4.4402
ξ	0.9583	0.4124	not relevant
Threshold condition	$R_0 \le \xi$	$\xi < R_0 < 1$	$R_0 > 1$
Stability of DFE	GAS	asymptotically stable (possibly co-exists with EE)	unstable

Table 3: Threshold numbers for the three sets of parameter values and the stability of DFE

	Description	Set 1	Set 2	Set 3
Humans				
Λ_h	immigration rate	0.041	0.03285	0.033
ψ_h	relative birth rate	5.5×10^{-5}	7.666×10^{-5}	1.1×10^{-4}
μ_{1h}	density-independent death/emmigration rate	8.8×10^{-6}	4.212×10^{-5}	1.6×10^{-5}
μ_{2h}	density-dependent death/emmigration rate	2×10^{-7}	10^{-7}	3×10^{-7}
σ_h	bites tolerated by a human per unit time	4.3	18	19
β_{hv}	probability of transmission of infection from infective mosquito	0.022	0.02	0.022
ν_h	transfer rate to infective $\frac{1}{\nu_h}$ = average duration of the latent period	0.1	0.08333	0.1
γ_h	recovery rate	0.0035	0.003704	0.0035
ρ_h	loss of immunity rate	0.0027	0.0146	0.00055
δ_h	disease-induced death rate	1.8×10^{-5}	3.454×10^{-4}	9×10^{-5}
Mosquitos				
ψ_v	relative birth rate	0.13	0.4	0.13
μ_{1v}	density-independent death rate	0.033	0.1429	0.033
μ_{2v}	density-dependent death rate	7×10^{-5}	2.279×10^{-4}	2×10^{-5}
σ_v	bites required by a mosquito per unit time	0.33	0.6	0.5
β_{vh}	probability of transmission of infection from infective human	0.24	0.8333	0.48
$\tilde\beta_{vh}$	probability of transmission of infection from recovered human	0.024	0.08333	0.048
ν_v	transfer rate to infective $\frac{1}{\nu_v}$ = average duration of the latent period	0.083	0.1	0.091

Table 2: Description of parameters and three sets of values used in numerical simulations

2 GAS results

Compact biologically feasible region:

$$\mathcal{G} = \left\{(\ S_h \quad E_h \quad I_h \quad R_h \quad S_v \quad E_v \quad I_v\ ) \in \mathcal{D};\ N_h^\# \le N_h \le N_h^*,\ N_v = N_v^*\right\} \qquad (10)$$

Theorem 1 *The set $\mathcal{G}$ in (10) is GAS for the dynamical system (1)–(7) defined on $\mathcal{D}$. (Thus, the study of the system (1)–(7) can be reduced from $\mathcal{D}$ to $\mathcal{G}$.)*

Following [3] for the model on $\mathcal{G}$, we have:

Theorem 2 *The DFE is GAS on $\mathcal{D}$ whenever*

$$R_0 \le \xi \qquad (11)$$

where

$$R_0 = c(N_h^*, N_v^*)\sqrt{\frac{\beta_{hv}\nu_h\nu_v\left(\beta_{vh} + \frac{\gamma_h + \tilde\beta_{vh}}{\rho_h + f_h(N_h^*)}\right) N_h^* N_v^*}{f_v(N_v^*)(\nu_h + f_h(N_h^*))(\nu_v + f_v(N_v^*))(\gamma_h + f_h(N_h^*) + \delta_h)}}. \qquad (12)$$

is the basic reproduction number and the additional threshold number ξ is given by

$$\xi = \sqrt{\frac{\sigma_h N_h^\# + \sigma_v N_v^*}{\sigma_h N_h^* + \sigma_v N_v^*} \times \frac{\nu_h + \mu_{1h} + \mu_{2h} N_h^\#}{\nu_h + \mu_{1h} + \mu_{2h} N_h^*} \times \frac{\gamma_h + \delta_h + \mu_{1h} + \mu_{2h} N_h^\#}{\gamma_h + \delta_h + \mu_{1h} + \mu_{2h} N_h^*} \times \frac{\beta_{vh} + \tilde\beta_{vh} \frac{\gamma_h}{\rho_h + \mu_{1h} + \mu_{2h} N_h^*}}{\beta_{vh} + \tilde\beta_{vh} \frac{\gamma_h}{\rho_h + \mu_{1h} + \mu_{2h} N_h^\#}}}.$$

Remark 3 *Since $\xi \le 1$, Theorem 2 is consistent with the bifurcation analysis in [2]: at $R_0 = 1$, there is forward bifurcation if $\delta_h = 0$ ($\xi = 1$) and possible backward bifurcationt if $\delta_h > 0$ ($\xi < 1$).*

3 A nonstandard finite difference scheme

Consider the following NSFD scheme in the sense of [1, 4]:

$$\begin{aligned}
\frac{S_h^{n+1} - S_h^n}{\phi(\Delta t)} &= \Lambda_h + \psi_h N_h^n + \rho_h R_h^{n+1} - c(N_h^n, N_v^n)\beta_{hv} I_v^n S_h^{n+1} - f_h(N_h^n) S_h^{n+1}, && (13)\\
\frac{E_h^{n+1} - E_h^n}{\phi(\Delta t)} &= c(N_h^n, N_v^n)\beta_{hv} I_v^n S_h^{n+1} - \nu_h E_h^{n+1} - f_h(N_h^n) E_h^{n+1}, && (14)\\
\frac{I_h^{n+1} - I_h^n}{\phi(\Delta t)} &= \nu_h E_h^{n+1} - (\gamma_h + f_h(N_h^n) + \delta_h) I_h^{n+1}, && (15)\\
\frac{R_h^{n+1} - R_h^n}{\phi(\Delta t)} &= \gamma_h I_h^{n+1} - \rho_h R_h^{n+1} - f_h(N_h^n) R_h^{n+1}, && (16)\\
\frac{S_v^{n+1} - S_v^n}{\phi(\Delta t)} &= \psi_v N_v^n - c(N_h^n, N_v^n)(\beta_{vh} I_h^n + \tilde\beta_{vh} R_h^n) S_v^{n+1} - f_v(N_v^n) S_v^{n+1}, && (17)\\
\frac{E_v^{n+1} - E_v^n}{\phi(\Delta t)} &= c(N_h^n, N_v^n)(\beta_{vh} I_h^n + \tilde\beta_{vh} R_h^n) S_v^{n+1} - \nu_v E_v^{n+1} - f_v(N_v^n) E_v^{n+1}, && (18)\\
\frac{I_v^{n+1} - I_v^n}{\phi(\Delta t)} &= \nu_v(t) E_v^{n+1} - f_v(N_v^n) I_v^{n+1} && (19)
\end{aligned}$$

where

$$\phi \equiv \phi(\Delta t) = \Delta t + O[(\Delta t)^2].$$

Dynamics consistency: The NSFD scheme is a discrete dynamical system on $\mathcal{D}$, which satisfies the discrete conservation laws

$$N_v^{n+1} = F_v(N_v^n) \qquad (20)$$

and

$$E_h(N_h^{n-1}) =: \underline{N}_h^n \le N_h^n \le \overline{N}_h^n := \overline{F}_h(N_h^{n-1}) \qquad (21)$$

where F_v, $\underline{E}_h$and $\overline{F}_h$ are suitable maps with the same fixed-points N_v^*, $N_h^\#$ and N_h^*, respectively, as for the continuous model, and

$$\phi(\Delta t) = (\Lambda_h \mu_{2h})^{-\frac{1}{2}}[1 - e^{-\Delta t(\Lambda_h \mu_{2h})^{\frac{1}{2}}}]. \qquad (22)$$

Theorem 4 *The set $\mathcal{G}$ in (10) is GAS for the discrete system (13)–(19) defined on $\mathcal{D}$ under the condition (22).*

Theorem 5 *The DFE is a GAS for the discrete dynamical system (13)–(19), with (22), on $\mathcal{D}$.*

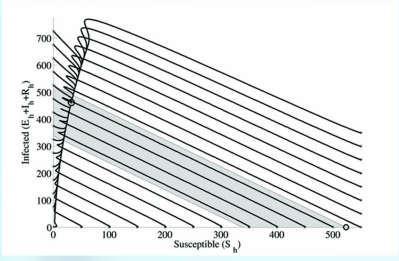

Figure 7: Unstable DFE: Parameter values from Table 2, Set 3.

4 Numerical simulations

Figures 2, 3 and 4 represent human population by compartment (left); total population, its lower bound $\underline{N}_h$ and its upper bound $\overline{N}_h$ in terms of (9) (right).

Figures 5, 6 and 7 provide phase diagrams of Infected or Disease Carriers ($E_h + I_h + R_h$) versus susceptible (S_h). The five pointed stars indicate the initial points of the trajectories. The shaded area is the projection of the set $\mathcal{G}$. An invariant manifold of one dimension less is clearly indicated on each figure. It is of interest to notice the coexistence of EE and DFE on figure 6. There are two asymptotically stable equilibria, denoted by circled stars and an unstable equilibrium denoted by a circle all within the region $\mathcal{G}$. This unstable equilibrium, which one can also see is a saddle point, actually accounts for the dip in the population size observed on Fig. 3.

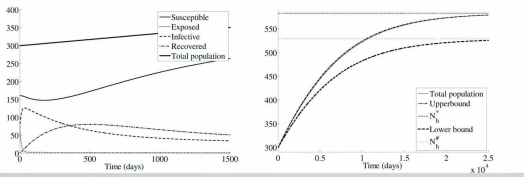

Figure 2: Parameter values from Table 2, Set 1: The rate of change of the compartments is eventually comparable with the rate of change of the total population (left). The solution approaches DFE (right). The total population remains between $\underline{N}_h$ and $\overline{N}_h$

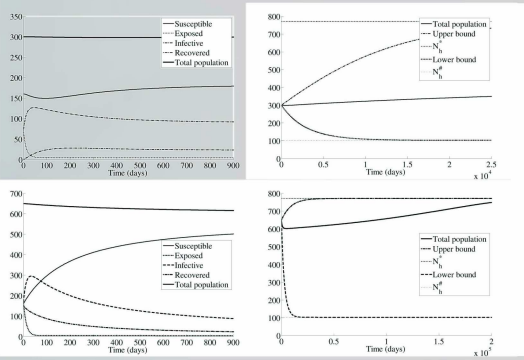

Figure 3: Parameter values from Table 2, Set 2: Two typical solutions are represented one converging to DFE (bottom) and one converging to an EE (top). In both cases the conservation law (9) is preserved (right). It is of interest to observe also the initial dip in the total population when the solution approaches DFE (bottom, right) which cannot be assimilated through a logistic equation.

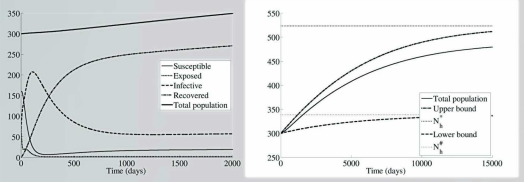

Figure 4: Parameter values from Table 2, Set 3: A typical solution initialed at a point outside the disease free manifold demonstrates that all such solutions converge to an EE.

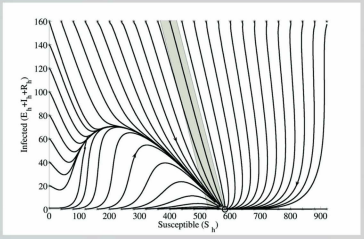

Figure 5: GAS of DFE: Parameter values from Table 2, Set 1.

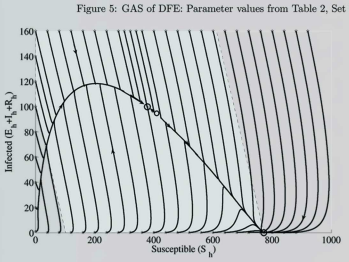

Figure 6: Backward bifurcation: Parameter values from Table 2, Set 2.

References

[1] R. Anguelov and J.M-S. Lubuma, Contributions to the mathematics of the nonstandard finite difference method and applications, *Numer. Methods Partial Differential Eq.* **17** (2001), 518–543.

[2] N. Chitnis, J.M. Cushin and J.M. Hyman, Bifurcation analysis of a mathematical model for Malaria transmission, *SIAM J. Applied Math.*, **67** (2006), 24–45

[3] J. C. Kamgang and G. Sallet, Computation of threshold conditions for epidemiological models and global stability of the disease free equilibrium , *Math. Biosc.* **213** (2008), 1–12.

[4] R. E. Mickens, *Nonstandard finite difference models of differential equations*, World Scientific, Singapore, 1994.